Talanta 118 (2014) 333–338

Contents lists available at ScienceDirect

Talanta

journal homepage: www.elsevier.com/locate/talanta

A facile approach to construct versatile signal amplification system for bacterial detection

Peng Qi [a,b], Dun Zhang [a,*], Yi Wan [a], Dandan Lv [a,b]

[a] Key Laboratory of Marine Environmental Corrosion and Bio-fouling, Institute of Oceanology, Chinese Academy of Sciences, 7 Nanhai Road, Qingdao 266071, China

[b] University of the Chinese Academy of Sciences, 19 (Jia) Yuquan Road, Beijing 100039, China

ARTICLE INFO

Article history:
Received 26 July 2013
Received in revised form
11 October 2013
Accepted 19 October 2013
Available online 29 October 2013

Keywords:
Signal amplification
Bacterial detection
Dopamine
Enhanced polymerization

ABSTRACT

In this work, a facile approach to design versatile signal amplification system for bacterial detection has been presented. Bio-recognition elements and signaling molecules can be immobilized on the surface of Fe_3O_4@MnO_2 nanomaterials with the help of bioinspired polydopamine (PDA). Fe_3O_4@MnO_2 nanoplates were chosen as carrier for bio-recognizing and signaling molecules because this kind of nanomaterial was superparamagnetic and the existence of MnO_2 could enhance the polymerization of dopamine due to its strong oxidative ability. This nanocomposite system was versatile because PDA around Fe_3O_4@MnO_2 nanoplates provided a stable and convenient platform for immobilization of biological and chemical materials, and various kinds of bio-recognizing and signaling molecules could be immobilized by reaction with pendant amino groups of dopamine to meet different detection requirements. Since a substantial amount of signaling molecules were immobilized on the surface of the nanocomposites, so the sensitivity of detection would be improved when the prepared nanocomposites were selectively conjugated with target pathogen. In the experimental section, a sandwich-type electrochemical biosensor was developed to verify the amplified bacterial detection sensitivity. Concanavalin A (conA) and ferrocene (Fc) were chosen as bio-recognition elements and signaling molecules for detection of *Desulforibrio caledoiensis*, respectively. The conA and Fc modified nanocomposites were conjugated on electrode by the selective recognition between conA and target bacteria, and the bacterial population was obtained by quantification of the electrochemical signal of Fc moieties. The experimental results showed that the detection sensitivity for *D. caledoiensis* was improved by taking advantage of this signal amplification system.

1. Introduction

The detection of bacteria is crucial to assess and avoid risks for both human health and environmental monitoring. Several methods have been reported in the field of bacterial detection, including the culture and colony counting methods, immunology-based methods, polymerase chain reaction (PCR) based methods, and biosensors [1]. The main advantages of biosensors, over the other bacterial detection methods, are rapid, cost-effective, and suitable for *in situ* analysis. Hence, biosensor has been widely studied for bacterial detection in recent years, and various techniques are being developed to improve the detection performance, such as selectivity and sensitivity.

Dopamine (2-(3,4-dihydroxyphenyl)ethylamine) is a kind of catecholamine neurotransmitter widely present in central nervous system. The dopamine molecular contains both catechol and amine functional groups, and it is susceptible to undergo oxidative polymerization process via a series of complex redox reactions under alkaline conditions [2]. Owing to the existence of pendant amino groups in the polymer, the polymerized dopamine provided an excellent platform for immobilization of biological and chemical molecules. In addition, thanks to the presence of ortho-dihydroxyphenyl structure, polydopamine (PDA) could be tightly bonded onto the surface of inorganic and organic materials [3]. Inspired by the biocompatibility of PDA and its versatile adhesion capability, dopamine polymerization process has been used to prepare of multifunctional coatings [4–7], biosensing platforms [8–11], nanocapsules for drug delivery [12], and functionalized inorganic nanomaterials [13,14]. For example, Zhao et al. [4] reported a material-independent and multifunctional modification protocol by PDA coating, and a convenient method for fabrication of CNTs with PDA has been proposed, and the resulting reactive PDA coating could be served as adhesion layer to immobilize metal nanoparticles and enzymes [15,16]. In our previous work, we have fabricated an immunosensor for nonlabeled detection of sulfate-reducing bacteria based on bioinspired PDA platform [10]. Recently, it has been reported that dopamine polymerization process could be induced and enhanced by the addition of oxidant [4,17]. This inspired us to investigate the polymerization of dopamine in the presence of

* Corresponding author. Tel./fax: +86 532 82898960.
E-mail addresses: zhangdun@qdio.ac.cn, zhangdun@ms.qdio.ac.cn (D. Zhang).

0039-9140/$ - see front matter © 2013 Elsevier B.V. All rights reserved.
http://dx.doi.org/10.1016/j.talanta.2013.10.040

MnO_2 nanomaterials, and we assumed that the strong oxidation ability of MnO_2 would enhance the polymerization reaction and a layer of PDA could be firmly adhered to the surface of the nanomaterials.

Herein, we presented a facile and versatile signal amplification system for bacterial detection. PDA was coated on the surface of Fe_3O_4@MnO_2 core–shell nanoplates by oxidative enhanced polymerization. We chose Fe_3O_4@MnO_2 core–shell nanomaterials for our research, because this composite nanomaterials are superparamagnetic at room temperature and the presence of MnO_2 can enhance the polymerization of dopamine due to its strong oxidative ability. PDA was firmly coated on Fe_3O_4@MnO_2 core–shell nanomaterials via chelation reaction, and the resulting PDA coated Fe_3O_4@MnO_2 (PDA-Fe_3O_4@MnO_2) nanoparticles supplied a stable platform for immobilization of chemical signal molecules, ferrocene (Fc), and recognizing elements, concanavalin A (ConA). ConA is a kind of carbohydrate binding lectin, which had a specific binding to mannosyl groups on bacterial membrane [18–20]. One kind of sulfate-reducing bacteria (SRB), *Desulforibrio caledoiensis*, was used as target bacteria, and the bacterial population was obtained by direct voltammetric analysis of Fc moieties. Since a substantial amount of Fc molecules was loaded on surface of PDA-Fe_3O_4@MnO_2 nanomaterials, the sensitivity of bacterial detection was largely improved (as shown in Fig. 1B). The presence of PDA on Fe_3O_4@MnO_2 core–shell nanomaterials facilitated the subsequent modification steps, and the other kinds of bio-recognizing and signaling molecules could be immobilized to meet different detection requirements. Hence, this work provided a facile and versatile approach to construct signal amplification system for bacterial detection.

2. Materials and methods

2.1. Chemicals

Dopamine hydrochloride (2-(3,4-Dihydroxyphenyl)ethylamine hydrochloride), 1-ethyl-3[3-dimethylaminopropyl] carbodiimide hydrochloride (EDC), bovine serum albumin (BSA) and freeze-dried Concanavalin A were purchased from Sigma-Aldrich. The conA solution was prepared with PBS containing 1 mM Ca^{2+} and 1 mM Mn^{2+} and stored at 4 °C. N-hydroxysuccinimide (NHS) and Ferrocenecarboxylic acid (Fc) were provided by Fluka. Polyvinyl pyrrolidone (PVP, K-30) was obtained from Beijing Solarbio science & Technology Co., Ltd., China. Other chemicals used in this paper were purchased from Sinopharm Chemical Reagent Co., Ltd., China. Milli-Q water (Millipore, USA) was used throughout.

2.2. Bacterial cultivation

The seed of target bacteria, *D. caledoiensis*, were isolated from marine bud of Bohai Sea, China. The bacterial cultivation and enumeration methods have been reported in our previous work [21–24]. Briefly, bacteria were cultivated in the modified Postgate's medium and visible bacterial number was determined according to American Society of Testing materials standard D4412-84. Bacterial cells were harvested through centrifugation (8000 rpm, 15 min) and rinsed with 0.2 M PBS. Bacterial solutions of various concentrations were obtained by serially dilution with PBS. *Staphylococcus aureus* and *Vibrio alginolyticus* were used as control microorganisms.

2.3. Preparation of Fe_3O_4@MnO_2 nanocomposites

The Fe_3O_4@MnO_2 core–shell nanoplates were synthesized through a facile and green hydrothermal method [25]. 100 mL deionized water was purged with nitrogen to remove oxygen before reaction, and then 2.5 mmol $FeSO_4$•$7H_2O$ and 1 g poly (vinylpyrrolidone) (PVP, K-30) were added into the deionized water and kept in a water bath at 90 °C for 1 h under gentle stirring. Afterwards, 1 mL 5.0 M NaOH aqueous solution was added to the solution, and the solution color changed to green rapidly. After 5 min of reaction, 2.5 mmol $KMnO_4$ was added into the mixture dropwisely, generating dark brown precipitates. The reaction solution was aged at room temperature for 12 h, and then the precipitates were filtered and thoroughly washed with water and ethanol alternately. Finally, the obtained products were dried in a vacuum at 50 °C for 24 h.

2.4. Preparation of PDA-Fe_3O_4@MnO_2 nanomaterials (PDA-Fe_3O_4@MnO_2)

The polymerization of dopamine was conducted in the presence of Fe_3O_4@MnO_2 nanoplates. 20 mg dopamine was added to 10 mL Tris–HCl buffer solution (pH 9.0) containing 0.2 mg mL^{-1} Fe_3O_4@MnO_2 nanoplates, and then the mixture was incubated in a glassy vial at room temperature under stirring. After a reaction time of 12 h, PDA-Fe_3O_4@MnO_2 were separated from the solution

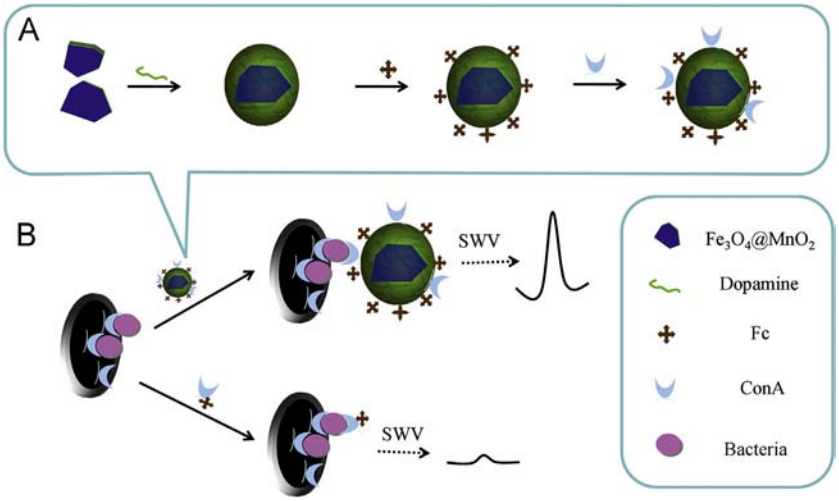

Fig. 1. Schematic representation of preparation of PDA-Fe_3O_4@MnO_2–Fc-conA nanocomposite and fabrication the sandwich-type Immunosensor with PDA-Fe_3O_4@MnO_2–Fc-conA based signal amplification (B).

though external magnetic field. Finally, PDA-Fe_3O_4@MnO_2 nanomaterials were washed with deionized water and redispersed in 10 mL Tris–HCl buffer and stored at 4 °C until use.

2.5. Preparation of conA and Fc modified PDA-Fe_3O_4@MnO_2 nanocomposites (PDA-Fe_3O_4@MnO_2–Fc-conA)

100 mM NHS and 400 mM EDC were added to 9 mL 10 μg mL^{-1} Fc solution and stirred for 4 h to activate the carboxyl groups of Fc. After that, 1 mL as-prepared PDA-Fe_3O_4@MnO_2 was added to the solution. After stirring for 12 h at room temperature, Fc moieties were conjugated onto the surface of PDA-Fe_3O_4@MnO_2 by reaction with the amino groups of PDA. PDA-Fe_3O_4@MnO_2–Fc were washed by centrifugation and then re-dispersed in 10 mL PBS. Next, 1 mL 2.5% glutaraldehyde was mixed with 1 mL PDA-Fe_3O_4@MnO_2–Fc solution. After stirring for 1 h, 1 mL 0.02 mg mL^{-1} conA solution was added into the mixture. The reaction was kept at room temperature for 24 h under stirring, and then PDA-Fe_3O_4@MnO_2–Fc-conA nanomaterials were harvested by centrifugation. After the washing treatment, PDA-Fe_3O_4@MnO_2–Fc-conA nanocomposites were re-dispersed in 1 mL PBS, and stored at 4 °C until use. The complete PDA-Fe_3O_4@MnO_2–Fc-conA fabrication process from Fe_3O_4@MnO_2 core–shell nanoplates was shown in Fig. 1A.

2.6. Preparation of Fc-conA

Fc-conA was prepared to verify the improvement of detection sensitivity. 9 mL 10 μg mL^{-1} Fc solution was mixed with 100 mM NHS and 400 mM EDC to active the carboxylic acid groups. After 4 h activation, 1 mL 0.2 mg mL^{-1} conA solution was added into the activated Fc solution, and the mixture was allowed to react for 12 h under stirring. Unreacted Fc was removed by dialysis in PBS, and the product was stored at 4 °C.

2.7. Fabrication of the immunosensor

A glassy carbon electrode (GCE) was polished to a mirror-like finish with 0.3 and 0.05 μm alumina slurry and thoroughly cleaned with ethanol and water. Then, the electrode was electrochemical modified in ethanol containing 0.1 M ethylenediamine and 0.1 M $LiClO_4$ by cyclic voltammetry from 0 to 1.4 V for 5 cycles at 20 mV s^{-1}. The resulting ethylenediamine monolayer modified GCE was soaked in water for 4 h to remove physical absorbed ethylenediamine. After that, the electrode was immersed in 0.5% glutaraldehyde for 1 h to active the amino groups of ethylenediamine and then thoroughly washed with water. ConA modified GCE (conA/GCE) was obtained by soaking the electrode into 0.1 mg mL^{-1} conA and incubated for 2 h at ambient conditions. Finally, the conA/GCE was incubated with 10 μL 1% BSA for 1 h to block non-specific binding sites on the electrode (BSA/conA/GCE). The well-prepared electrode was stored at 4 °C until use.

Fig. 1B shows the bacterial detection procedures of the electrochemical immunosensors in the presence and absence of signal amplification system. Firstly, BSA/conA/GCE was incubated with 10 μL drop of bacterial solutions for 1 h at ambient conditions, followed by washing with PBS (Bacteria/BSA/conA/GCE). Next, 10 μL of PDA-Fe_3O_4@MnO_2–Fc-conA solution was added on the surface of the electrode and incubated for 1 h. PDA-Fe_3O_4@MnO_2–Fc-conA was immobilized on the electrode surface by selectively reaction between conA and the target bacteria (PDA-Fe_3O_4@MnO_2–Fc-conA/Bacteria/BSA/conA/GCE). After thoroughly washing, the electrode was ready for electrochemical measurements. In the control experiment, Fc-conA instead of PDA-Fe_3O_4@MnO_2–Fc-conA was added to verify the detection sensitivity enhancement.

2.8. Electrochemical measurements

Electrochemical measurements were carried out with a CHI 760C Electrochemical Workstation (CH instruments, Inc., Shanghai). All electrochemical experiments were performed with the immunosensing electrode as working electrode, a Pt wire as counter electrode, and an Ag/AgCl electrode as reference electrode. Electrochemical impedance spectroscopy (EIS) was used to characterize the stepwise modification process of working electrode. EIS was performed in 0.2 M PBS containing 5 mM $[Fe(CN)_6]^{4-/3-}$ redox couple at open circuit potential and the amplitude of applied sinusoidal wave potential was 10 mV in the frequency range of 0.1 Hz to 100 kHz. Bacterial population was detected by recording the redox process of Fc species absorbed on the immunosensing electrode, using Square Wave Voltammetry (SWV). SWV measurements were performed in PBS and the following parameters were used, initial potential 100 mV, final potential 600 mV, scan increment 4 mV, pulse height 25 mV, and frequency 25 Hz.

3. Results and discussion

3.1. Characterization of Fe_3O_4@MnO_2 core–shell nanoplates

The formation mechanism of Fe_3O_4@MnO_2 core–shell nanoplates has been clearly illustrated in the literature [25]. Transmission electron microscopic (TEM) images showed that the magnetic

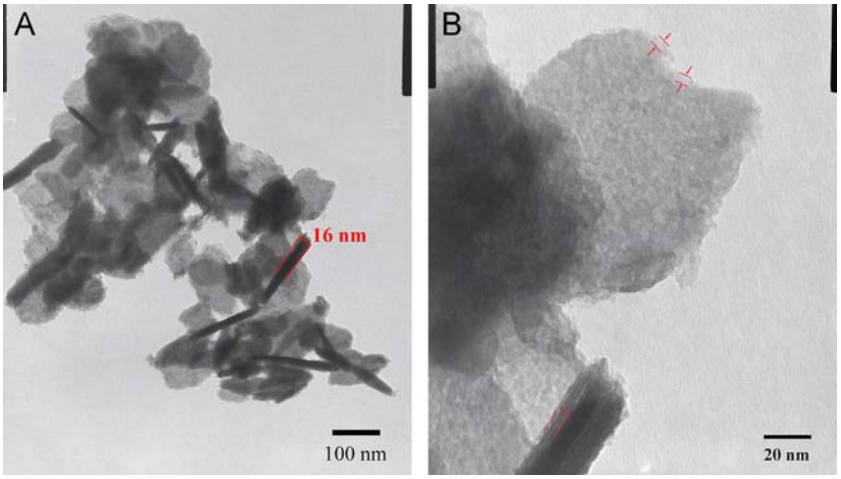

Fig. 2. TEM images of Fe_3O_4@MnO_2 nanoplates at different magnification.

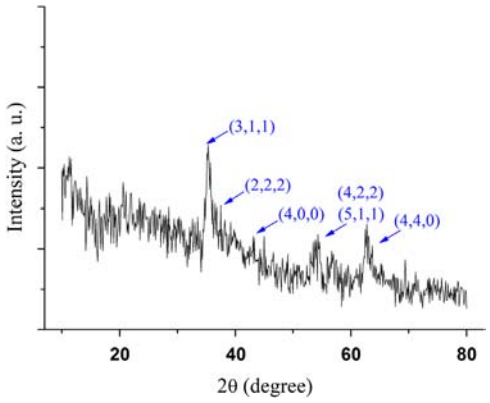

Fig. 3. XRD pattern of Fe_3O_4@MnO_2 nanoplates.

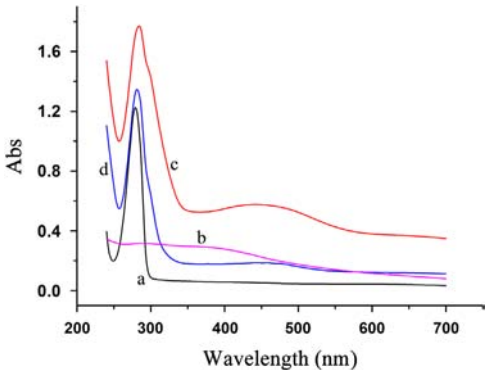

Fig. 4. The UV–vis absorption spectra of dopamine hydrochloride (a), Fe_3O_4@MnO_2 nanoplates (b), and PDA samples in the presence (c) and absence (d) of Fe_3O_4@MnO_2 nanomaterials.

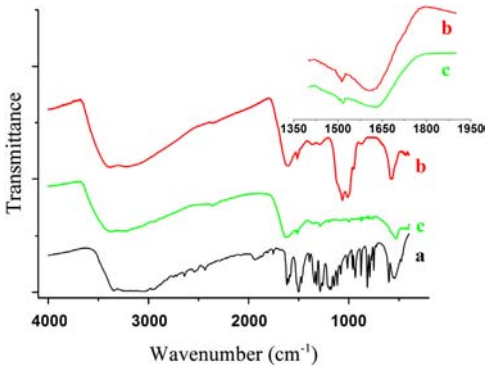

Fig. 5. FTIR spectra of dopamine hydrochloride (a) and PDA samples in the presence (b) and absence (c) of Fe_3O_4@MnO_2 nanomaterials.

core–shell nanoplates with a thickness of about 16 nm were aggregated. The rod-shaped morphologies represented the vertical standing nanoplates. As seen from Fig. 2B, a layer of MnO_2 amorphous shell was uniformly formed on the surface of crystalline Fe_3O_4 core with the thickness of about 3 nm. The amorphous MnO_2 was produced from the following routes, *in situ* reduction of $KMnO_4$ by $FeSO_4$, reaction between $KMnO_4$ and PVP, and the decomposition of excess $KMnO_4$. Because of the presence of hydroxyl radicals on the surface, MnO_2 could firmly adhere to Fe_3O_4 cores [25].

XRD result showed that Fe_3O_4 has a face-centered cubic crystal structure, while there is no visible crystalline peak was detected for MnO_2. The broad peak located at $2\theta=22^\circ$ in XRD pattern confirmed the amorphous nature of MnO_2 (Fig. 3). Fe_3O_4@MnO_2 core–shell structure was chosen for our research, because this kind of composite nanomaterial was superparamagnetic at room temperature, so it could be used for magnetic separation. Furthermore, the presence of MnO_2 in the nanocomposites could enhance the polymerization of dopamine due to its strong oxidative nature.

3.2. Characterization of PDA-Fe_3O_4@MnO_2 nanomaterials

Polymerization of dopamine was conducted in Tris–HCl buffer solution (pH 9.0) in the presence and absence of Fe_3O_4@MnO_2 nanoplates. UV–vis spectroscopy was used to characterize the polymerization process, and the results were shown in Fig. 4. Before polymerization, only a characteristic peak of dopamine was observed at 280 nm [26] (curve a), and there was no absorption peak in Fe_3O_4@MnO_2 nanoplates (curve b). After 12 h of reaction in the presence of Fe_3O_4@MnO_2 nanomaterials, the absorption intensity of dopamine increased and a broad peak was developed at 480 nm (curve c). This absorption peak was assignable to a characteristic transition of chrome formation, and the peak intensity was considered as an indicator of the polymerization degree [4]. A stronger absorption intensity at 480 nm corresponded to a higher degree of polymerization. Effect of Fe_3O_4@MnO_2 nanoplates on polymerization of dopamine could be obtained from Fig. 4. Compared with the UV–vis spectrum of the polymerized dopamine solution in the absence of Fe_3O_4@MnO_2 nanomaterials (curve d), the dopamine sample polymerized in the presence of Fe_3O_4@MnO_2 nanomaterials showed stronger absorption intensity (curve c). This result indicated that dopamine polymerization process was enhanced by the addition of Fe_3O_4@MnO_2 nanoplates. The reason for the enhancement was that MnO_2 was a strong oxidizing agent and the catechol groups on dopamine would undergo a polymerization process under oxidative conditions [4,27].

Fourier transform infrared (FTIR) spectroscopy was used to characterize PDA-Fe_3O_4@MnO_2 nanomaterials. Fig. 5 displayed the FTIR spectra of dopamine hydrochloride, PDA samples with and without the enhancement of Fe_3O_4@MnO_2 nanomaterials. Dopamine hydrochloride showed a broad and strong band in the 3000–3400 cm^{-1} region, resulting from hydroxyl structures as well as water. Compared with dopamine hydrochloride, two absorption peaks were observed at 1515 and 1605 cm^{-1} in both PDA samples. These two absorption peaks were assignable to the indole structure formed during dopamine polymerization [28,29]. Besides, absorption features of carbonyl structures in dopamine hydrochloride were obscured in two PDA samples because of intramolecular cyclization reaction and formation of indole derivatives. Comparing the spectra of the two PDA samples, PDA sample polymerized in the presence of Fe_3O_4@MnO_2 nanomaterials exhibited absorption peaks around 1000 cm^{-1}, which is owing to the coordination between the catechol oxygens of dopamine and MnO_2. Therefore, PDA could be firmly attached to the surface of Fe_3O_4@MnO_2 nanoplates, and PDA-Fe_3O_4@MnO_2 nanomaterials provided a stable platform for further functionalization.

3.3. Fabrication of immunosensor

A sandwich-type electrochemical biosensor was constructed as described in Section 2.7. ConA moieties were immobilized onto the electrode surface with the help of ethylenediamine. Electrochemical deposition of ethylenediamine was conducted by cyclic voltammetry for 5 cycles from 0 to 1.4 V at 20 mV s^{-1} in ethanol containing 0.1 M ethylenediamine and 0.1 M $LiClO_4$. Fig. 6 shows the cyclic voltammetric curves during ethylenediamine modification. A broad, irreversible oxidation peak was observed at 1.1 V, which was corresponded to the oxidation of amine group to its corresponding cation radical. This result was consistent with earlier literature about oxidation of amines on carbon-based electrodes [30,31]. After scanning for 5 cycles, an ethylenediamine monolayer was formed on the surface of GCE.

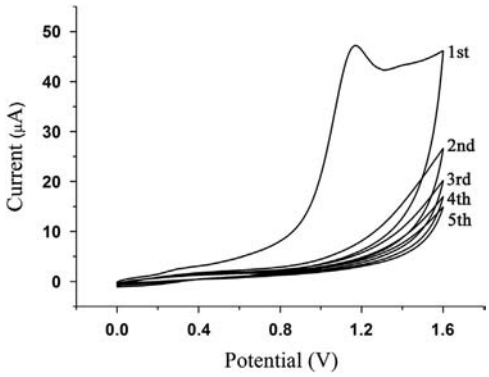

Fig. 6. Voltammetric behavior of ethylenediamine deposition at 20 mV s^{-1} for 5 cycles in ethanol containing 0.1 M ethylenediamine and 0.1 M $LiClO_4$.

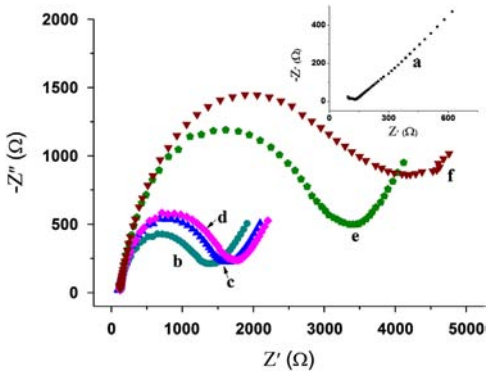

Fig. 7. Impedance spectra of bare GCE (a), ethylenediamine modified GCE (b), conA/GCE (c), BSA/conA/GCE (d), Bacteria/BSA/conA/GCE (e), and PDA-Fe_3O_4@MnO_2–Fc-conA/Bacteria/BSA/conA/GCE (f) obtained in PBS containing 5 mM $[Fe(CN)_6]^{4-/3-}$ redox couple. The bacterial concentration was 1.0×10^7 cfu mL^{-1}.

EIS was used to characterize the stepwise modification of functionalized electrode. The Faradic impedance spectra of $[Fe(CN)_6]^{4-/3-}$ during the immunosensor fabrication process were shown in Fig. 7. In Faradic impedance spectra, the diameter of semicircle represents the magnitude of charge transfer resistance (R_{ct}) of $[Fe(CN)_6]^{4-/3-}$ towards electrode surface. R_{ct} is the most sensitive and straightforward parameter used to characterize electrode fabrication process. Compared with bare GCE electrode (curve a), R_{ct} increased after a monolayer of ethylenediamine was formed on the surface of GCE (curve b), because the ethylenediamine layer retarded the charge transfer process of redox $[Fe(CN)_6]^{4-/3-}$. ConA molecules could also hinder the charge transfer process, so a larger resistance was observed when conA was covalently modified on the electrode (curve c). Curve d represents the impedance response of redox couple $[Fe(CN)_6]^{4-/3-}$ on the surface of BSA/conA/GCE. The well fabricated immunosensor can selectively bind with the target bacteria, which lead to an increase of R_{ct} response (curve e). After incubated with signal amplification group, PDA-Fe_3O_4@MnO_2–Fc-conA, the charge transfer process of redox $[Fe(CN)_6]^{4-/3-}$ was further hindered, leading to the increase of impedance response (curve f).

3.4. Bacterial detection performance

To certify the improvement of detection sensitivity, conA-Fc and PDA-Fe_3O_4@MnO_2–Fc-conA labels were used to construct sandwich immunoassays, respectively. These two signal labels can selectively bind with the target bacteria by the interaction between conA and the mannosyl groups on bacterial membrane. We hypothesized the detection sensitivity could be improved by

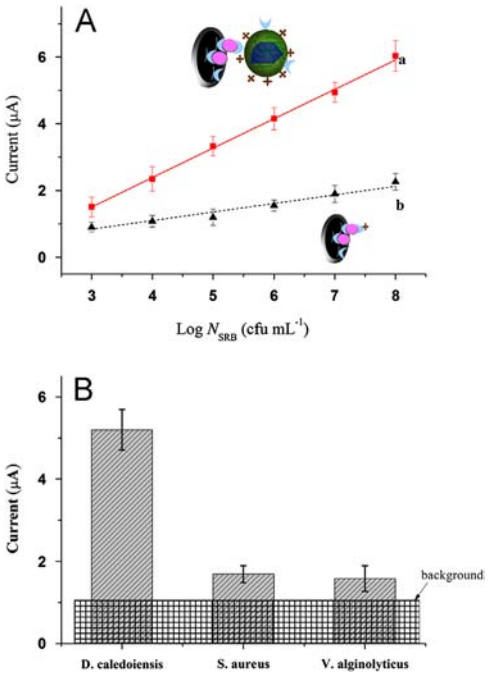

Fig. 8. (A) Comparison of the standard curves produced using PDA-Fe_3O_4@MnO_2-Fc-conA (a) or conA-Fc (b) as electrochemical label. (B) Specificity of the bacterial detection method, the bacterial concentration of *D. caledoiensis*, *S. aureus* and *V. alginolyticus* was 10^7 cfu mL^{-1}.

using PDA-Fe_3O_4@MnO_2–Fc-conA, since electrochemical signal was obtained from Fc redox current and the amount of Fc molecules modified on the surface of PDA-Fe_3O_4@MnO_2 nanomaterials was substantial. Fig. 8A shows the SWV responses of the immunosensor towards target bacteria of various concentrations. Anodic current was used after subtracting the background current. As seen in Fig. 8A, the peak current was increased proportional to the logarithm of bacterial concentration in the range of 1×10^3 to 1×10^8 cfu mL^{-1}. Comparing the two sets of data, the SWV responses were enhanced when PDA-Fe_3O_4@MnO_2–Fc-conA was used as signal label. The detection sensitivity of the proposed signal amplification system was 0.881 μA (Log cfu $mL^{-1})^{-1}$, while the slope for conA-Fc label was only 0.256 μA (Log cfu $mL^{-1})^{-1}$, the sensitivity enhancement was on the order of 340%, suggesting PDA-Fe_3O_4@MnO_2–Fc-conA was an effective signal amplification system.

The other detection parameters of the immunosensor were also investigated. *aureus* and *Vibrio alginolyticus* were used as control microorganisms to evaluate the detection selectivity (the result was shown in Fig. 8B). The selectivity was realized by taking advantage of conA, and *D. caledoiensis* produced a significantly higher electrochemical signal than that of the control. 10^6 cfu mL^{-1} of *D. caledoiensis* was measured five times to investigate the reproducibility of the developed immunosensor. The relative standard deviation (RSD) was 4.3%, suggesting acceptable reproducibility and precision of this system.

4. Conclusions

In summary, this work described a new and simple method to construct signal amplification system based on PDA-mediated nanomaterial modification. Polymerization of dopamine was enhanced by addition of Fe_3O_4@MnO_2 nanoplates, and PDA formed on the surface of Fe_3O_4@MnO_2 nanomaterials facilitated the immobilization of Fc and conA. When PDA-Fe_3O_4@MnO_2–Fc-conA was immobilized on electrode surface by the specific

interaction between conA and the target bacteria, the electrochemical signal was increased because the amount of Fc label anchored on PDA-Fe_3O_4@MnO_2–Fc-conA was great. The greatest strengths of the signal amplification system based on PDA-mediated nanomaterials modification were simple and versatile, other chemical or biological labels and bio-recognition elements could be immobilized according to different detection requirements.

Acknowledgments

This work was supported by the National Natural Science Foundation of China (Grant no. 41306072 and 41076047), Science & Technology Basic Research Program of Qingdao (Grant no. 13-1-4-181-jch) and the Shandong Provincial Natural Science Foundation, China (Grant no. ZR2010DM004).

References

[1] V. Velusamy, K. Arshak, O. Korostynska, K. Oliwa, C. Adley, Biotechnol. Adv. 28 (2010) 232–254.
[2] Y. Tan, W. Deng, Y. Li, Z. Huang, Y. Meng, Q. Xie, M. Ma, S. Yao, J. Phys. Chem. B 114 (2010) 5016–5024.
[3] H. Lee, N.F. Scherer, P.B. Messersmith, Proc. Natl. Acad. Sci. USA 103 (2006) 12999–13003.
[4] Q. Wei, F. Zhang, J. Li, B. Li, C. Zhao, Polym. Chem. 1 (2010) 1430–1433.
[5] B.D. McCloskey, H.B. Park, H. Ju, B.W. Rowe, D.J. Miller, B.J. Chun, K. Kin, B.D. Freeman, Polymer 51 (2010) 3472–3485.
[6] H. Lee, J. Rho, P.B. Messersmith, Adv. Mater. 21 (2009) 431–434.
[7] H. Lee, S.M. Dellatore, W.M. Miller, P.B. Messersmith, Science 318 (2007) 426–430.
[8] M. Li, C. Deng, Q. Xie, Y. Yang, S. Yao, Electrochim. Acta 51 (2006) 5478–5486.
[9] F. Li, Y. Feng, L. Yang, L. Li, C. Tang, B. Tang, Biosens. Bioelectron. 26 (2011) 2489–2494.
[10] Y. Wan, D. Zhang, Y. Wang, P. Qi, B. Hou, Biosens. Bioelectron. 26 (2011) 2595–2600.
[11] T.A. Morris, A.W. Peterson, M.J. Tarlov, Anal. Chem. 81 (2009) 5413–5420.
[12] B. Yu, D.A. Wang, Q. Ye, F. Zhou, W. Liu, Chem. Commun. 44 (2009) 6789–6791.
[13] H. Peng, R. Liang, L. Zhang, J. Qiu, Biosens. Bioelectron. 42 (2013) 293–299.
[14] M. Zhang, X. He, L. Chen, Y. Zhang, J. Mater. Chem. 20 (2010) 10696–10704.
[15] Y. Wang, L. Liu, M. Li, S. Xu, F. Gao, Biosens. Bioelectron. 30 (2011) 107–111.
[16] B. Fei, B. Qian, Z. Yang, R. Wang, W.C. Liu, C.L. Mak, J.H. Xin, Carbon 46 (2008) 1795–1797.
[17] R. Ouyang, J. Lei, H. Ju, Chem. Commun. (2008) 5761–5763.
[18] Z. Shen, M. Huang, C. Xiao, Y. Zhang, X. Zeng, P.G. Wang, Anal. Chem. 79 (2007) 2312–2319.
[19] Q. Lu, H. Lin, S. Ge, S. Luo, Q. Cai, C.A. Grimes, Anal. Chem. 81 (2009) 5846–5850.
[20] B. Bondurant, J.A. Last, T.A. Waggoner, A. Slade, D.Y. Sasaki, Langmuir 19 (2003) 1829–1837.
[21] P. Qi, Y. Wan, D. Zhang, Biosens. Bioelectron. 39 (2013) 282–288.
[22] P. Qi, D. Zhang, Y. Wan, Sens. Actuators, B-Chem. 181 (2013) 274–279.
[23] Y. Wan, D. Zhang, B. Hou, Biosens. Bioelectron. 25 (2010) 1847–1850.
[24] Y. Wan, Y. Wang, J. Wu, D. Zhang, Anal. Chem. 83 (2011) 648–653.
[25] Z. Zhao, J. Liu, F. Cui, H. Feng, L. Zhang, J. Mater. Chem. 22 (2012) 9052–9057.
[26] W.J. Barreto, S. Ponzoni, P. Sassi, Spectrochim. Acta A 55 (1999) 65–72.
[27] B.P. Lee, J.L. Dalsin, P.B. Messersmith, Biomacromolecules 3 (2002) 1038–1047.
[28] D.R. Dreyer, D.J. Miller, B.D. Freeman, D.R. Paul, C.W. Bielawski, Langmuir 28 (2012) 6428–6435.
[29] D.G. Osullivan, J. Chem. Soc. (1960) 3278–3284.
[30] R.S. Deinhammer, M. Ho, J.W. Anderegg, M.D. Porter, Langmuir 10 (1994) 1306–1313.
[31] C.K. Mann, Anal. Chem. 36 (1964) 2424–2426.